ELSEVIER

Polymer 41 (2000) 4599–4605

polymer

Phase differentiation of a tri-phase polymer composite using energy-filtering transmission electron microscopy

K. Varlot[a,*], J.M. Martin[a], C. Quet[b]

[a]*Ecole Centrale de Lyon, Laboratoire de Tribologie et Dynamique des Systèmes UMR 5513, BP 163, 69131 Ecully Cedex, France*
[b]*Elf Atochem, Groupement de Recherches de Lacq, BP 34, 64170 Artix, France*

Received 31 May 1999; received in revised form 30 August 1999; accepted 13 September 1999

Abstract

Energy-filtering transmission electron microscope (EFTEM) in the image-spectrum mode was used to differentiate the phases in a tri-phase polymeric composite (PS/PB/PMA), by imaging characteristic chemical bondings. Although the sample suffered irradiation damage, image acquisition was performed on it at ambient temperature for convenience. The mapping of polystyrene (PS) was easily obtained from the $\pi \rightarrow \pi^*$ transition at 7 eV, a characteristic of the undamaged aromatic ring. Poly(methyl acrylate) (PMA) was imaged using the C $1s \rightarrow \pi^*$(C=C) transition at 284.8 eV from damaged residues, with the elemental mapping revealing oxygen artifacts due to irradiation damage. Finally, the polybutadiene (PB) phase could be directly imaged, only after staining with osmium tetroxide, through the elemental mapping of osmium.

This work shows that it is possible to differentiate the phases of an unstained polymeric composite at a sub-micron scale. A reasonable interpretation of the filtered images must, however, be based on a perfect understanding of the polymer degradation processes. This technique will be particularly useful to map the distribution of organic additives inside the polymer, such as peroxides. © 2000 Elsevier Science Ltd. All rights reserved.

Keywords: Polymer; Composite; Energy-filtering transmission electron microscope

1. Introduction

One of the most common methods for observing polymer composites, transmission electron microscopy (TEM), often includes the use of a selective stain, generally either OsO_4 (osmium tetroxide) or RuO_4 (ruthenium tetroxide). This procedure incorporates in the polymer sample atoms of high atomic number, whose increased probability of elastic scattering enhances contrast. In this sense, it can be either a physical or a chemical incorporation. Yet, chemical reactions are preferred since physically adsorbed atoms (iodine for example) may vaporize under vacuum. Osmium and ruthenium are the most common stains for polymer imaging. Fixation is a chemical cross-linking (see Fig. 1), and causes an increase in the density and changes the chemical properties of the polymer. Unfortunately, the chemical cross-linking may modify the phases geometrically (shrinkage of the stained phase).

The most commonly used stains are listed in Table 1. Osmium and ruthenium react with several functional groups. Phase differentiation in a composite is based on preferential absorption (a qualitative method). In a polystyrene/polybutadiene/poly(methyl methacrylate) (PS/PB/PMMA) composite, for example, it is known that ruthenium reacts preferentially with PB, this phase appearing dark in conventional TEM imaging (CTEM). Ruthenium fixes less on the aromatic group in PS than on the ethylenic carbon double bonds in PB (polybutadiene), so PS is gray. Finally, the PMMA carbonyl group does not react with ruthenium tetroxide and that phase remains white.

The main advantage of the staining procedure is to rigidify the polymer. In the case of high-impact PS for example (PS matrix with inclusions of PB, which give a better impact resistance), osmium react only with PB. The working temperature in ultramicrotomy was defined by the transition temperature of PB (about $-80°C$ for unstained PB). After staining, cross-linking between chains increases the transition temperature of PB above ambient temperature; which avoids hard working conditions for the specimen preparation.

As mentioned above, phase differentiation in a composite is qualitative, since it is based on the preferential absorption

* Corresponding author. Tel.: + 33-472-43-62-09; fax: +33-472-43-85-28.

E-mail address: karine.varlot@insa-lyon.fr (K. Varlot).

0032-3861/00/$ - see front matter © 2000 Elsevier Science Ltd. All rights reserved.
PII: S0032-3861(99)00684-9

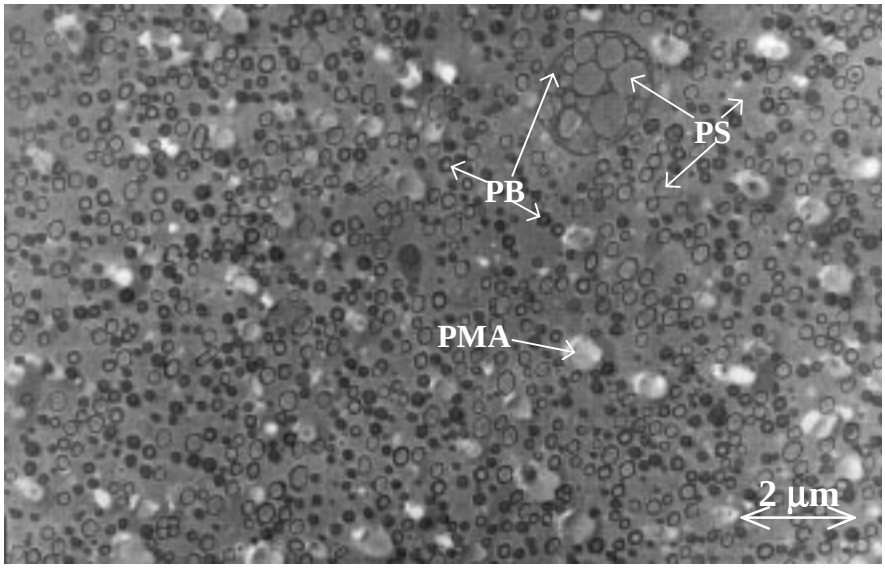

Fig. 1. CTEM micrograph of the tri-phase composite. The specimen was stained with ruthenium tetroxide to give more contrast. Ruthenium was prefentially fixed on PB and makes this phase appear dark (strong abosrption on ethylenic C=C double bonds). PS appears grey (weak absorption on aromatic rings) and PMA remains white (no absorption on carbonyl groups).

of the stain on functional groups. In the case of multiphase composites, this can lead to mistakes. Moreover, the appearance of artifacts linked to chemical modification of the stained phase and the accompanying shrinkage can occur, and is not well understood. Moreover, the stain reacts with the polymer (cross-linking between polymeric chains) by modifying the chemical structure; a chemical analysis of the phases is useless. With the view to analyze chemically the polymeric phases, it is important to avoid changes in the chemical structure during specimen preparation. Unstained polymers are used here preferentially.

Chemical imaging of unstained polymeric composites has already been investigated with the synchrotron radiation: thanks to its excellent energy resolution, X-ray microscopy is a powerful technique to study the distribution of polymer phases. Good contrast images could even be obtained on PC/PET composites, although PC and PET have similar chemical structures [1]. However, with the view to analyze interfaces, the spatial resolution in X-ray microscopy is not sufficient. A few attempts to obtain the distribution of polymeric phases at higher spatial resolution were done in the TEM [2–4], but generally using elemental mapping, instead of chemical bonding mapping. This is only possible with polymer blends, where each phase has a characteristic element.

In this paper, we want to demonstrate the capability of chemical bonding mapping using energy-filtered TEM (EFTEM), more precisely in the image-spectrum mode. Therefore, we chose a composite, in which the phases have characteristic chemical bondings. The chemical bondings lead to certain characteristic features of the energy-loss spectrum.

2. Materials and methods

The tri-phase composite is a commercial product of Sumitomo (DJ8000) and is composed of PS, PB and PMA (poly(methyl acrylate)). Its composition was determined by combining infrared spectroscopy and TEM on stained pellets. A micrograph of the polymer after staining with ruthenium tetroxide is displayed in Fig. 1. Its structure is close to that of high-impact PS, with a PS matrix and

Table 1
Most commonly used compounds for selective staining of polymers

Functional groups	Examples	Stains
–CH–CH–	Saturated hydrocabons (PE, PP)	Chlorosulfonic acid phosphotungstic acid ruthenium tetroxide
–C=C–	Unaturated hydrocarbons (PB)	Osmium tetroxide ruthenium tetroxide ebonite
–OH, –COH–	Alcohols, aldehydes	Osmium tetroxide ruthenium tetroxide silver sulfide
–O–	Ethers	Osmium tetroxide ruthenium tetroxide
$–NH_2–$	Amines	Osmium tetroxide ruthenium tetroxide
–COOR	Esters (polyesters)	Phosphotungstic acid silver sulfide methanolic NaOH
$–CONH_2$, –CONH–	Amides (nylon)	Phosphotungstic acid tin chloride
Aromatic rings	PS, PET	Ruthenium tetroxide silver sulfide mercury trifluoroacetate

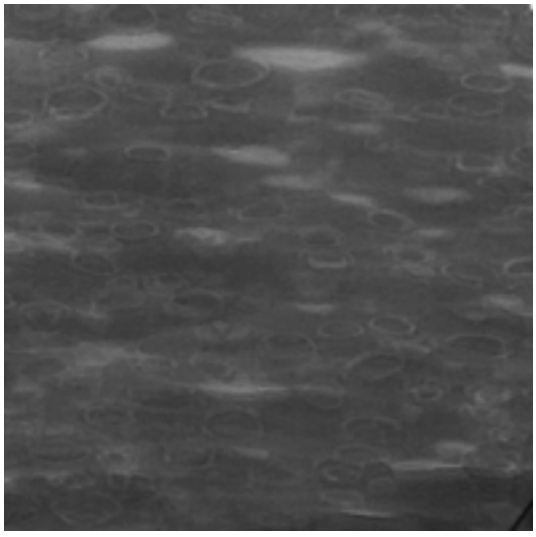

Fig. 2. Zero-loss filtered image of the PS/PB/PMA composite acquired on the Philips CM200/GIF microscope at ambient temperature.

capsules of PS coated with PB, but with extra large inclusions of PMA.

Pellets of the tri-phase polymeric composite were microtomed at a low temperature (Ultracut E from Reichert–Jung), just below the glass transition temperature of PB (about −90°C). The sections about 50-nm-thick were placed on top of 400-mesh copper grids. Unlike homogeneous polymer sections previously analyzed by EELS [5], copper grids were not covered by holey carbon films to avoid stress in the polymer due to the electron beam, because these holey carbon films would have lead to artifacts in the filtered images (thickness effects).

Two different microscopes were used to perform chemical imaging of polymeric composites:

- *Philips CM200/GIF*. The accelerating voltage was set to 200 kV. The microscope was equipped with a Gatan energy-filter placed under the column. A slit at the entrance of the spectrometer limited the spectrum to a particular energy-loss ΔE. The filtered image was detected by a CCD camera (1024×1024 photodiodes). In the ESI mode, the slit was set to 20 eV to have a good signal/noise ratio. The acquisition time for an image at the oxygen K-edge (532 eV) was about 30 s. In the image-spectrum mode, the slit was set to 5 eV, which is close to the limit of the system, for detecting any signal.
- *Zeiss 902*. The accelerating voltage was 80 kV. The microscope was equipped with a Castaing–Henry filter inside the column. Filtered images were acquired using a low-light camera (Dage SIT1000). The acquisition time per image was just a few seconds, even when the slit was set to 3 eV. This allowed us to acquire filtered images of the chemical bondings at the carbon K-edge with a good signal/noise ratio.

Unfortunately, the electron dose received by the specimen could not be calculated. Therefore, the assignment of the fine structure and the critical dose for great irradiation damage were based on previous experiments with homogeneous polymers using EELS [6–8].

3. Results and discussion

The zero-loss micrograph obtained with a slit centered on $\Delta E = 0$ might give interesting results. Unfortunately, as all the unstained phases were composed of light elements (low Z) at about the same concentration, no increase of contrast was observed (see Fig. 2). As the specimen was amorphous, contrast in the zero-loss image can be attributed to thickness variations. Low contrast therefore shows that thickness variations are small. In the following discussion, they will be neglected and the filtered images will not be divided by the zero-loss image (to reduce the artifacts caused by thickness variations [9]).

As far as charged polymers are concerned, energy filtering images of the charges is only based on the nature of the elements. ESI with a large slit is a well-suited method for obtaining, quickly, elemental mapping of the charges with a good signal-to-noise ratio. On the contrary, in the case of the filtered images of an unstained polymeric composite, it is necessary to consider the fine structure of each phase. In the case of the PS/PB/PMA tri-phase composite, the characteristic signature at negligible irradiation damage includes:

- The presence of a $\pi \rightarrow \pi^*$ peak at 6.9 eV in PS and not in the other phases, assigned to the excitation of the aromatic ring.
- The presence of oxygen in only the PMA phase.
- The absence of neither characteristic in the PB phase. From the EELS signatures of the three phases, PB was then thought to be the most difficult phase to image without any staining procedure.

3.1. Identification of PS

A Philips CM200/GIF microscope was used to acquire filtered images with low energy loss. In order to reduce the effect of irradiation damage, the acquisition was reduced to two images (ESI mode). The peak at 6.9 eV, which has been attributed to the excitation of the aromatic ring in PS, indeed disappeared with increasing electron dose (critical electron dose: 10^3 C m^{-2}) [6]. However, the specimen was kept at ambient temperature in order to test the capabilities of EFTEM on electron-sensitive materials with user-friendly conditions. These two conditions are not incompatible, because acquiring filtered images requires a decondensed beam and therefore a reduced electron dose is received by the specimen.

The image of the aromatic ring of the PS phase is displayed in Fig. 3. It was obtained by subtracting of the images acquired at $\Delta E = 7$ and at 2 eV, respectively. The

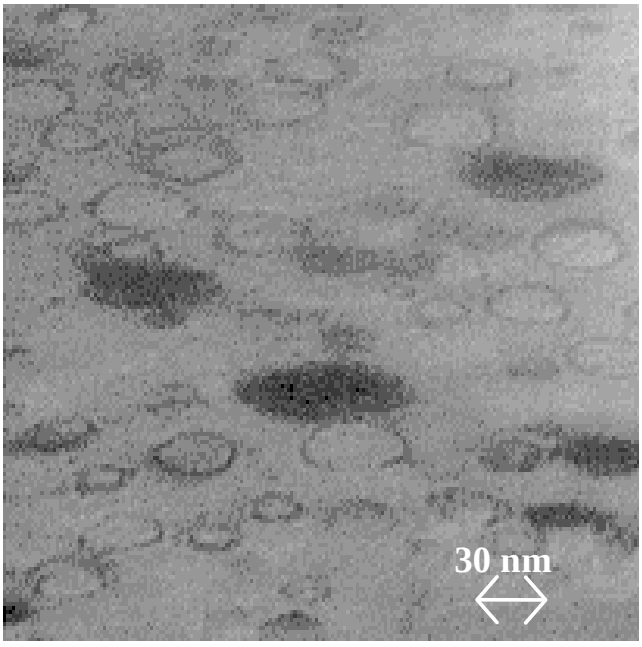

Fig. 3. Distribution of the aromatic rings in PS. It was obtained by subtracting the image at 7 eV by the image at 2 eV. PS forms both the matrix and the inside of the capsules. Microscope Philips CM200/GIF; slit 5 eV; ESI mode; ambient temperature.

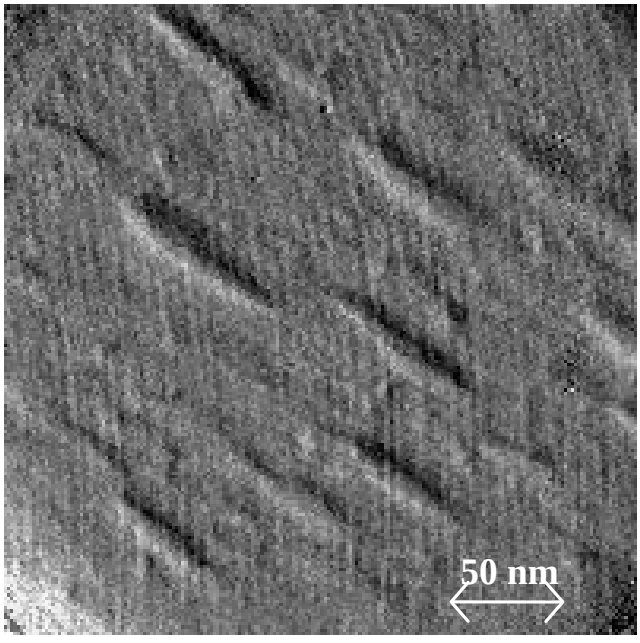

Fig. 4. Elemental mapping of oxygen in the tri-phase polymeric composite (three-image subtraction assuming a power-law background). Due to irradiation damage (breakage of carbonyl groups in PMA), the oxygen K-edge can hardly be detected, which gives very noisy filtered images. Moreover, even after correction of the specimen drift with a precision of 1/4 pixel, shadowing can be observed. Microscope Philips CM200/GIF; slit 20 eV; ESI mode; ambient temperature.

calculated image shows the distribution of the aromatic ring and therefore of PS. Both the matrix and the inside of the capsules are composed of PS. Irradiation damage (marked by a disappearance of the peak at 7 eV) is not a major problem for acquiring such filtered images at ambient temperature, because the signal to noise ratio is very good in the plasmon region.

3.2. Identification of PMA

Even for the identification of the PMA phase, we first wanted to keep the specimen at the ambient temperature (a convenient working condition for the microscopist). Irradiation damage is very important in PMA and affects the oxygen-to-carbon ratio (breakage of the carbonyl group). The critical electron dose is so small that even after cooling the specimen to liquid nitrogen temperature ($-196^{\circ}C$), the acquisition of a spectrum without any irradiation damage is impossible. Therefore, the acquisition at the oxygen K-edge was set to two images (ESI mode) with a large slit in order to increase the signal to noise ratio and detect a small fraction of residual oxygen. In these conditions, the acquisition time with the Philips CM200/GIF microscope was about 30 s, which means that the PMA phase was degraded during the acquisition of the first image. The following discussion considers the process of irradiation damage of PMA.

The filtered image of oxygen is displayed in Fig. 4 (three-image subtraction assuming a power-law background). The brighter phase should be PMA, but the signal to noise ratio is poor and some shadowing can be seen in the image. This can usually be attributed to a drift of the specimen during the acquisition of the images acquired at various energy-losses, but all three images were drift-corrected to a precision of 1/4 pixel. It is impossible to determine whether the observed shadowing is due to irradiation damage, an artifact of the acquisition system or to the heterogeneity in the specimen.

Another way to image the PMA phase is to focus on the carbon K-edge near-edge structure. For negligible irradiation damage, PMA presents a sharp peak around 289 eV, which can be assigned to a C $1s \rightarrow \pi^{*}$(COO) [8]. Unfortunately, this peak disappears at great irradiation damage, since many of the carbonyl groups are destroyed. Filtered images of this chemical bonding, indeed, did not show any characteristic features of the PMA phase. The PMA phase was degraded during the acquisition of the images and the peak could not be detected.

When considering the degradation process of all phases, we could obtain a contrast with the PMA phase appearing brighter (see Fig. 5). This filtered image was obtained by subtraction, in the second derivative mode of the image at $\Delta E = 285$ eV by the image at $\Delta E = 276$ eV. For negligible irradiation damage, PS indeed shows a strong peak at 284.8 eV, characteristic of the aromatic ring, whereas this peak is only present in PB with a medium area (fewer ethylenic double bonds) and is completely absent in PMA (which lacks C=C

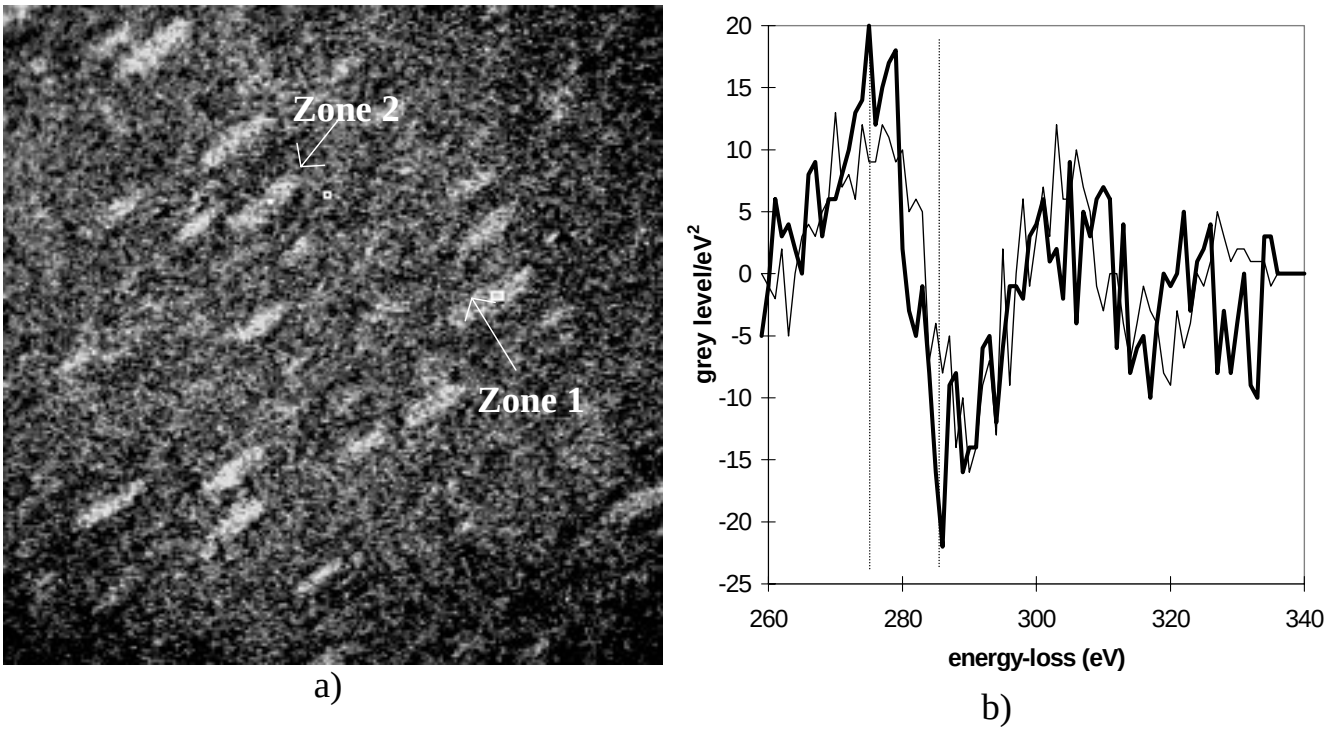

Fig. 5. (a) Distribution of C=C double bonds in the tri-phase polymeric composite and (b) spectra, in the second derivative mode, extracted from the filtered serie. PMMA appears brighter because after great irradiation damage, the peak C 1s → π*(C=C) at 284.8 eV is larger in both area and height than for PS and PB. Microscope Zeiss 902; slit 3 eV; image-spectrum mode, with subtraction of the image at 285 eV by the image at 276 eV in the second derivative mode.

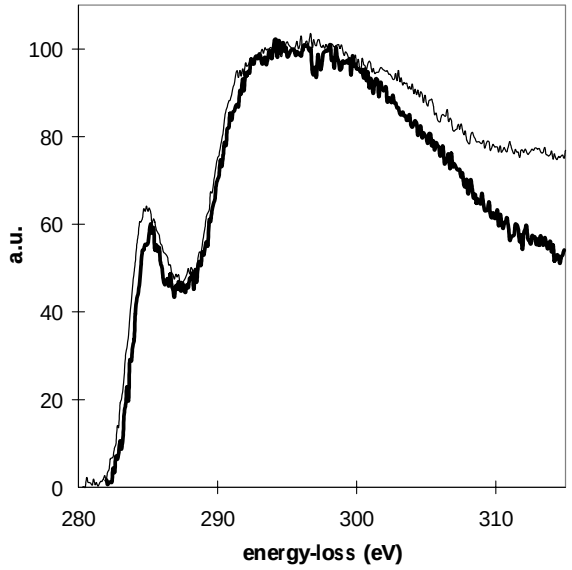

Fig. 6. EELS spectra, after great irradiation damage at each phase. The spectra were normalized at 294 eV, where the fine structure is thought to be negligible. The peak at 284.8 eV, assigned to a transition towards π*(C=C) orbitals, is slightly more intense for PMA than for the other phases (no difference between PS and PB). This explains the contrast in Fig. 5. Microscope Philips EM420/PEELS, STEM mode; spot size 50 nm; energy dispersion 0.1 eV/channel; resolution:1.0 eV FWHM measured on the zero-loss peak; ambient temperature.

double bonds). With increasing electron dose, degradation modifies the carbon K-edge fine structure as follows:

- In PS, the aromatic ring is destroyed, as seen from the disappearance of the peak at 6.9 eV ($\pi \rightarrow \pi^*$ transition of the aromatic ring) and the appearance of peaks at lower energy ($\pi \rightarrow \pi^*$ transition of ethylenic C=C double bonds, the energy depending on the number of conjugated bonds) [6]. At the carbon K-edge, destruction of the aromaticity causes a decrease in, both, the area and height of the peak at 284.8 eV. At the same time, the peaks at 291.1 and 293.2 eV, respectively, corresponding to transitions towards σ^*(C–C) of the main chain and of the aromatic ring change in intensity, the first one becoming predominant with increasing electron dose.
- In PB, more C=C bonds are created by dehydrogenation, leading to the formation of a conjugated polymer. At the carbon K-edge, the peak at 284.8 eV increases in area and in height, whereas the peak at 287.4 eV (transition towards a mixed Rydberg/σ^*(C–H)) disappears [5].
- The degradation process of PMA was not studied in detail but we can say that it is close to that of PMMA [5]. The only difference should lie in the kinetics of the first phase (dehydrogenation and formation of C=C double bonds), since PMA has two adjacent hydrogen linked to carbon atoms, which makes the dehydrogenation easier. The first phase caused a fast increase of the peak at 284.8 eV (transition 1s → π*(C=C)). The

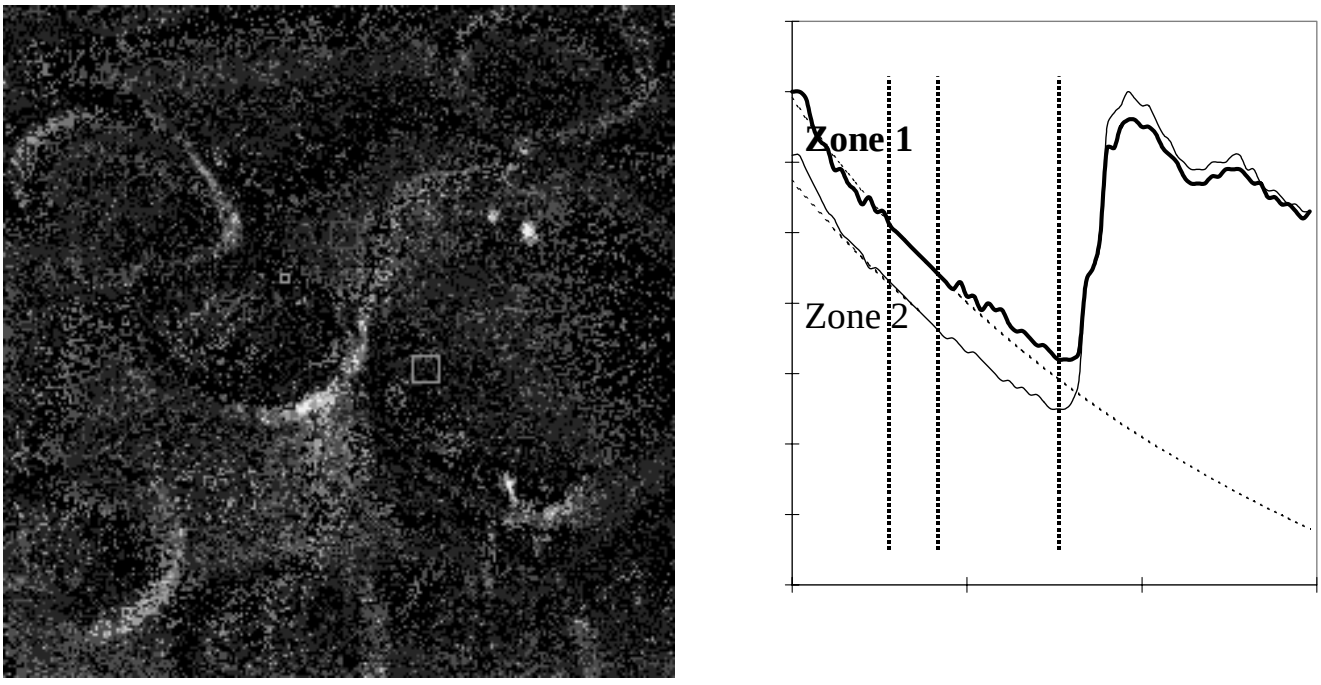

Fig. 7. (a) Elemental mapping of osmium (three-image subtraction assuming a power-law background) in the polymeric composite, slightly stained with osmium tetroxide and (b) spectra extracted from the filtered series. The calculated background is also displayed. Osmium reacts only with the ethylenic C=C double bonds in PB. The osmium elemental mapping is therefore equivalent to the distribution of PB. Only the coating of the capsules appears bright. Microscope Zeiss 902; slit 3 eV; image-spectrum mode, on the Os $N_{4,5}$-edge.

electron dose received by the polymer was usually too high to observe the first phase of the degradation process. In the second phase, carbonyl groups were broken. This was seen on the EELS spectrum as a decrease of the oxygen to carbon ratio, and also as a disappearance of the peak at 288 eV (transition $1s \rightarrow \pi^*(COO)$) and a further increase of the peak at 284.8 eV.

Comparing with EELS, the fine structure at the carbon K-edge in the different phases, the intensity of the peak at 284.8 eV after great irradiation damage was found slightly greater in PMA than in the other phases (no visible differentiation of PS and PB, see Fig. 6). This confirms that the filtered image in Fig. 5 gives the distribution of the PMA phase through the distribution of C=C double bonds after great irradiation damage, note that the inclusions were distorted in the cutting direction (in fact there was no rigidification since there was no incorporation of stain).

3.3. Identification of PB

The PB phase is undoubtedly the most difficult phase to image in a composite: PB does not show any strong feature on its EELS spectrum and it is present in the composite only in very thin layers (dark when stained, see Fig. 1).

From the previous results, we can deduce that the coating of the capsules was indeed composed of PB, since this area contained neither aromatic rings nor many C=C double bonds after great irradiation damage. A detailed study of each phase during irradiation damage may reveal characteristic features in the low-loss part of the EELS spectrum. Further work might indicate whether the PB phase inside polymeric composites could be illuminated in filtered images.

An alternative, to the study of the fine structure, is to stain lightly the polymeric composite with osmium tetroxide. Osmium tetroxide indeed gets fixed on only the ethylenic C=C double bonds in PB, and does not perturb the aromatic ring in PS nor the carbonyl groups in PMA. The distribution of the PB phase therefore corresponds to the distribution of osmium. We focused on the osmium $N_{4,5}$-edge at 273 eV, usually detected as a change of slope in the background before the carbon K-edge. The elemental mapping of osmium is displayed in Fig. 7, and is a representative of PB in the polymeric composite. Only the capsule coating appears to be bright. In the future, one might use a slightly selective staining to reveal interfaces or defaults in polymeric composites.

4. Conclusion

We have performed EFTEM experiments (both ESI and image-spectrum modes) on a tri-phase polymeric composite without staining, in order to chemically differentiate the phases. This is the first step towards the analysis of polymeric interfaces at high spatial resolution. EFTEM is a

powerful tool for polymer imaging, both for elemental mapping (distribution of mineral additives) and chemical bonding mapping (differentiation of the phases). However, with the present acquisition times, it is necessary to have a complete understanding of the irradiation damage process of polymers. The interpretation of filtered images must be based on degraded polymers. Good results were, however, obtained at ambient temperature, i.e. at convenient conditions. Further advance in chemical imaging of polymers should necessarily consider a reduction in the electron dose.

An alternative to the reduction of the electron dose may consist in slightly staining the sample so that the polymer chemistry and the phase structure are almost unaffected by the staining procedure (which will allow a chemical characterization of the composite phases), and the high-Z atom concentration is sufficient to perform elemental mapping.

References

[1] Ade H, Smith AP, Zhang H, Zhuang GR, Kirz J, Rightor E, Hitchcock AP. X-ray microscopy in polymer science: prospects of a *new* imaging technique. Polymer 1995;36(9):1843.

[2] Horiuchi S, Yase K, Kitano T, Higashida N, Ougizawa T. Energy-filtering transmission electron microscopy for the characterization of polymer blend morphologies. Pol J 1997;29(4):380.

[3] Duchesne A, Lieser G, Wegner G. Electron spectroscopic imaging-techniques for the investigation of multiphase polymer systems: poly-(styrene-b-methylphenylsiloxane) thin films. Colloids and Pol Sci 1994;272:1329.

[4] Hunt J, Disko MM, Behal SK, Leapman RD. Electron energy-loss chemical imaging of polymer phases. Ultramicroscopy 1995;58:55.

[5] Varlot K. Apport de la microscopie électronique filtrée en énergie (TEM/EELS) à la caractérisation chimique des polymères. PhD thesis, Ecole Centrale de Lyon, France, 1998, No.98-45.

[6] Ritsko JJ, Bigelow RW. Core excitons and the dielectric responde of polystyrene and poly(2-vinylpyridine) from 1 to 400 eV. J Chem Phys 1978;69:4162.

[7] Varlot K, Martin JM, Quet C. Physical and chemical changes in polystyrene during electron irradiation using EELS in the TEM. Contribution of the dielectric function. J Mic 1998;191(2):187.

[8] Varlot K, Martin JM, Gonbeau D, Quet C. Chemical bonding analysis of electron-sensitive polymers by EELS. Polymer 1999;40(20):5691.

[9] Egerton RF. Electron energy-loss spectroscopy in the electron microscope, 2. New York: Plenum Press, 1996.